Improved Differential Attacks for ECHO and Grøstl *

Thomas Peyrin

Ingenico, France
thomas.peyrin@ingenico.com

Abstract. We present improved cryptanalysis of two second-round SHA-3 candidates: the AES-based hash functions ECHO and Grøstl. We explain methods for building better differential trails for ECHO by increasing the granularity of the truncated differential paths previously considered. In the case of Grøstl, we describe a new technique, the internal differential attack, which shows that when using parallel computations designers should also consider the differential security between the parallel branches. Then, we exploit the recently introduced Super-Sbox attacks, that proved to be very efficient when attacking AES-like permutations, to achieve a very efficient utilization of the available freedom degrees. Finally, we obtain the best known attacks so far for both ECHO and Grøstl. In particular, we are able to mount a distinguishing attack for the full Grøstl-256 compression function or internal permutations.

Key words: hash function, cryptanalysis, ECHO, Grøstl, AES, internal differential attack.

1 Introduction

Cryptographic hash functions are very important tools in cryptography, used in many applications such as digital signatures, authentication schemes or message integrity. Informally, a hash function H is a function that takes an arbitrarily long message as input and outputs a fixed-length hash value of size n bits. The classical security requirements for such a function are collision resistance and (second)-preimage resistance. Namely, it should be impossible for an adversary to find a collision (two distinct messages that lead to the same hash value) in less than $2^{n/2}$ hash computations, or a (second)-preimage (a message hashing to a given challenge) in less than 2^n hash computations. Moreover, those primitives are traditionally used to simulate the behavior of a random oracle [2] and while the community is divided on such a requirement, in the ideal case an attacker should not be able to distinguish a hash function from a random oracle.

As many standardized hash functions [31, 41] have been broken a few years ago [44, 45], the NIST launched in 2008 the SHA-3 competition [33] that will lead to the future hash function standard. 14 candidates among 51 have been selected for the second round and many of them (like ECHO [3], Grøstl [14] or SHAvite-3 [5]) are actually using some parts of the standardized block cipher AES [10,32] as internal primitives or mimicking the structure of this cipher. While AES-256 can no more be considered as secure in the related-key model [7], the cryptography community has made important progresses concerning the evaluation of AES-based hash functions security [15, 19, 23, 25–27, 35]. Those attacks make an extensive use of the freedom degrees that are available in a hash function and even provides the best known distinguishing attack against AES-128 [15] in the known-key model [21,30]. Much recent analysis of AES-based hash functions has helped to identify the limits of current techniques, but as we show in this paper, it is possible to improve the differential path building methods used so far.

* This is the extended and corrected version of the article published at CRYPTO 2010. Concerning ECHO, the differential paths have been corrected and the memory requirements improved. Concerning Grøstl, hash function collision attack on reduced versions have been added together with a more general and improved internal differential technique providing more freedom degrees for the compression function distinguishers.

Our contributions. In this paper, we improve the best known cryptanalysis results [1, 15, 18, 26, 27] on two second round SHA-3 candidates: the hash functions ECHO [3] and Grøstl [14]. While we do not provide advances regarding the freedom degrees optimization, we use the recently introduced Super-Sbox techniques [15, 23] in order to find pairs of inputs verifying a given differential path. We then exploit some specific properties of ECHO and Grøstl to derive very good differential paths. More precisely, we improve the previously known truncated differential paths for ECHO by reducing the size of the truncated words considered. This allows us to broaden the differential trail search space, therefore increasing our probability to find a good path, but also augmenting the search complexity. We circumvent this constraint by giving a heuristic method to prune the potential candidates. Concerning Grøstl, we describe a novel yet simple cryptanalysis technique: the *internal differential attack*. It may be applied for functions using parallel branches that are not sufficiently made distinct. In that case, the attacker can find input instances (where a classical differential attack exhibits pairs of inputs) verifying non random properties on the output.

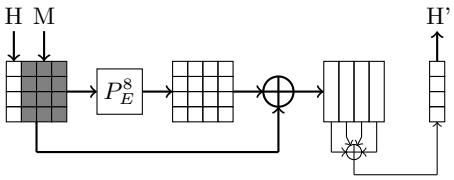

ECHO

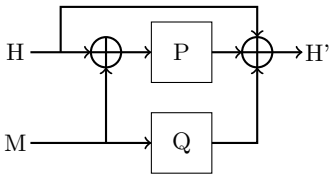

Grøstl

As a result, we improve the complexity for distinguishing the internal permutation of ECHO from a random 2048-bit permutation for a number of rounds corresponding to the full 256-bit version. Because of the folding phase after the permutation application at the end of the ECHO compression function, this attack does not translate into a distinguishing attack for the full ECHO compression function, nor the hash function itself. We provide also the first distinguishing attack on the full internal permutations for the 256-bit version of Grøstl, which can be directly derived into a distinguisher on the full Grøstl-256 compression function. Structural distinguishers (independent of the number of rounds) were already described in the original submission document [14]. For example, it was already identified that one can find fixed points or build a distinguisher for the compression function with the generalized birthday paradox [43]. However, our results also allow to distinguish the Grøstl compression function from the same construction when assuming the two internal permutations P and Q as ideal. This is not the case for the known structural distinguishers since they already consider the two internal permutations as ideal. Our results are also interesting because they exploit the specificities of P and Q which is essential in order to really evaluate the security margin of this hash function in terms of number of rounds. Finally, this also shows that the permutations P and Q used in Grøstl-256 can not be considered as ideal permutations. Because of its output function, this attack does not translate into a distinguishing attack for the full Grøstl hash function.

All the results and the corresponding computation/memory complexities for ECHO, ECHO-SP (the simple-pipe version of ECHO) and Grøstl are summarized in Table 1. The results concerning the internal permutation of ECHO are given in Appendix. Note that none of the results described in this article seem to endanger the security of the ECHO compression function or the Grøstl hash function.

2 Previous cryptanalysis

In this section, we recall the recent advances regarding cryptanalysis of AES-like permutations and their specificities. In the rest of the paper, we will use the Super-Sbox attacks as basic tool for finding input pairs verifying a given differential path.

Table 1. Summary of results for ECHO, ECHO-SP and Grøstl compression functions. ECHO-256, ECHO-SP-256, ECHO-512 and ECHO-SP-512 compression functions have 8, 8, 10 and 10 rounds respectively, while Grøstl-256 and Grøstl-512 compression functions have 10 and 14 rounds respectively.

target	rounds	computational complexity	memory requirements	type	section
ECHO-256 comp. function	3	2^{64}	2^{32}	free-start collision	5.2
	3	2^{96}	2^{32}	semi-free-start collision[1]	5.2
	4.5	2^{96}	2^{32}	distinguisher	5.1
ECHO-512 comp. function	3	2^{96}	2^{32}	(semi)-free-start collision[1]	5.2
	6.5	2^{96}	2^{32}	distinguisher	5.1
ECHO-SP-256 comp. function	3	2^{64}	2^{32}	(semi)-free-start collision	App. C
	3	2^{64}	2^{32}	distinguisher	App. C
ECHO-SP-512 comp. function	3	2^{64}	2^{32}	free-start collision	App. C
	3	2^{96}	2^{32}	semi-free-start collision[1]	App. C
	4.5	2^{96}	2^{32}	distinguisher	App. C
Grøstl-256 internal permutation	9	2^{80}	2^{64}	distinguisher	5.3
	10	2^{192}	2^{64}	distinguisher	5.3
Grøstl-512 internal permutation	11	2^{640}	2^{64}	distinguisher	5.3
Grøstl-256 comp. function	8	2^{112}	2^{64}	distinguisher	see [15]
	9	2^{80}	2^{64}	distinguisher[2]	5.3
	10	2^{192}	2^{64}	distinguisher[2]	5.3
Grøstl-512 comp. function	11	2^{640}	2^{64}	distinguisher[2]	5.3
Grøstl-256 hash function	4	2^{64}	2^{64}	collision	see [28]
	5	2^{79}	2^{64}	collision	5.4
Grøstl-512 hash function	5	2^{176}	2^{64}	collision	see [28]
	6	2^{177}	2^{64}	collision	5.4

2.1 Building differential trails with truncated differences

Cryptanalysis of AES-based hash functions began with the hash family proposal Grindahl [20] for which collision attacks have been found [19,35]. This showed that truncated differentials [20,22] are very useful when cryptanalyzing a byte-oriented primitive such as the AES. Namely, instead of looking at the actual difference value of a byte, one only checks if a byte contains a difference (active byte) or not (inactive byte). In particular, this allows the attacker to handle the non-linear Sboxes quite nicely when building differential trails. On the other hand, the differential transitions through the linear MixColumns layer will now be verified probabilistically.

The matrix multiplication underlying the MixColumns transformation on a r-byte column for AES or Grøstl presents the interesting property of being a Maximum-Distance Separable (MDS) mapping: the number of active input and output bytes is always greater or equal to $r+1$ (unless there is no active input and output byte at all). When picking random inputs, the probability of success of a differential transition that meets the MDS constraints through a MixColumns layer is determined by the number of active bytes in the output. More precisely, if such a differential transition contains k active bytes in one column of the output, its probability of success will approximatively be equal to $2^{-8\times(r-k)}$. For example, a $4 \mapsto 1$ transition for one column of the AES MixColumns layer has success probability of approximatively 2^{-24}. Note that the same reasoning applies when dealing with the invert function of the MixColumns layer as well.

[1] Because of a lack of freedom degrees, these attacks requires some randomization on the salt or counter input. Thus they are applicable in the chosen-salt or chosen-counter setting only.

[2] For these distinguishers, the amount of available freedom degrees allows us to generate only one valid candidate with good probability.

2.2 Rebound attacks

The rebound attack [27] is a new technique for using efficiently the available freedom degrees. The authors utilize truncated differential paths in which most of the cost lies in the middle rounds. Then, by using a local meet-in-the-middle-like technique, the freedom degrees are consumed in the middle part of the differential path, right where they can improve at best the overall complexity. More precisely, some rounds in the middle (the *controlled rounds*) will be verified with only a few operations on average, while the rest of the path both in forward and backward direction (the *uncontrolled rounds*) is fulfilled probabilistically. This cryptanalysis provides good results [23, 25] and can work without any special constraint on the differential path. However, the controlled part is limited to two rounds.

2.3 Start-from-the-middle attacks

In [26], the start-from-the-middle attack for AES-like permutations is introduced. It can be seen as a generalization of the previous technique in the sense that the idea is simply to use the freedom degrees for AES-like permutations in the "most expensive" part of the differential trail, without setting any constraint in the way this is handled. The "cheaper" parts are then covered in an inside-out manner in both forward and backward directions. The authors describe a freedom degrees use example that can control 3 rounds in the middle part, without increasing the complexity (i.e. with only a few operations). However, the depicted technique only works for specific differential paths, in which the number of active bytes in the controlled rounds is not too important. We refer to the original publication [26] for more details.[1]

2.4 The Super-Sbox cryptanalysis technique

Finally, another example of start-from-the-middle attacks is the Super-Sbox cryptanalysis ([15] and independently published in [23]). The idea is that one can view two rounds of an AES-like permutation as the parallel application of a layer of big Sboxes, named Super-Sboxes, preceded and followed by simple affine transformations. This technique can control 3-rounds in the middle of the differential trail with only a few operations on average, but works especially when the number of active bytes in the controlled rounds is important (this allowed to use longer differential paths which generally contain more active bytes). Because of some local precomputation steps, the drawback of this technique is its memory requirement when the size of the internal state of the scheme is too big. In the case of Grøstl this remains acceptable with a 2^{64} memory requirement, but in the case of ECHO as much as 2^{512} memory is required, making this tool unsuitable for this hash proposal. We refer to the original article [15] for more details.

3 Improved differential attack for ECHO

3.1 Description of ECHO

ECHO is a double-pipe hash function using HAIFA [4] as chaining iteration mode. The message to hash is first padded and divided into fixed-length blocks M_i which are used to update iteratively the chaining variable H_i (originally initialized with an initial vector $H_0 = IV$) thanks to the compression function h: $H_i = h(H_{i-1}, M_i)$. Finally, the hash output is obtained by truncating the last chaining variable. The compression function is built upon a 2048-bit AES-like permutation P_E^R composed of R rounds and its internal state can be viewed as a 4×4 matrix of 128-bit words (or cells). A cell will be denoted by $C_{i,j}$, where i is its row position and j its column position in the matrix, starting the counting from 0. One round of P_E^R is composed of three layers: the "BIG SubBytes" layer (big Sbox or B.SB), the "BIG ShiftRows" layer (B.ShR) and the "BIG MixColumns" layer (B.MC).

[1] Unlike claimed in [26], it seems that this technique can not be applied to ECHO, because of the 128-bit size of the AES-like cells.

The BIG SubBytes layer is a non-linear function defined by the application of a big Sbox S on each 128-bit cell and this big Sbox is made of 2 AES rounds. The classical AddRoundKey part from the AES is not present in P_E^R and in order to avoid trivial symmetric vulnerabilities that would occur, each big Sbox in ECHO is distinct thanks to different subkey additions in each of the 2-round AES uses. The first round subkey depends on the value of a 64-bit internal counter K that is different at each use, while the second round subkey is set to the 128-bit salt value and thus always remains the same during the whole ECHO computation. So, for each cell $C_{i,j}$ of the internal state, we compute

$$C'_{i,j} = S[C_{i,j}] = AES_{salt}(AES_{0||K}(C_{i,j})).$$

where AES_{sk} denotes the application of one AES round with the subkey sk. As for the AES, the BIG ShiftRows transformation permutes the position of each cell in its own row: for each cell $C_{i,j}$ of the internal state, we compute $C'_{i,j} = C_{i,Sub_i(j)}$ where $Sub_i(j) = (j-i) \bmod 4$. Finally, the BIG MixColumns function is a linear function that mixes all the columns of the internal state separately. More precisely, the 32-bit AES MixColumns function is reused: if $C^b_{i,j}$ denotes the b-th byte of the cell $C_{i,j}$, then we compute

$$({C'}^b_{0,j}, {C'}^b_{1,j}, {C'}^b_{2,j}, {C'}^b_{3,j}) = AESMixColumns(C^b_{0,j}, C^b_{1,j}, C^b_{2,j}, C^b_{3,j})$$

for all $0 \leq j \leq 3$ and $1 \leq b \leq 16$. The round function on an internal state C can thus be defined as:

$$MixColumns \circ ShiftRows \circ SubBytes(C).$$

In the case of the ECHO-256 compression function, 8 rounds of the permutation are applied and a folding phase is processed after the final feedforward. Namely, the folding phase (denoted fold_{256}) xors all the four 512-bit columns together. Finally, the compression function takes a 1536-bit message input M (12 words) and a 512-bit chaining variable input H (4 words) and outputs a new 512-bit chaining variable H' with

$$H' = \mathsf{fold}_{256}(P_E^8(H||M) \oplus H||M)$$

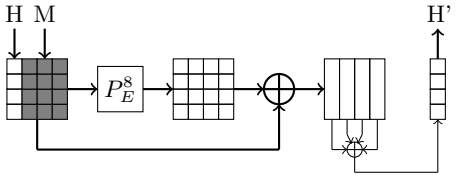

In the case of the ECHO-512 compression function, 10 rounds of the permutation are applied in order to turn a 1024-bit message input M (8 words) and a 1024-bit chaining variable input H (8 words) onto a new 1024-bit chaining variable H'. A different folding phase is processed after the final feedforward. Namely, the folding phase (denoted fold_{512}) xors the two first and the two last 512-bit columns together.

$$H' = \mathsf{fold}_{512}(P_E^{10}(H||M) \oplus H||M)$$

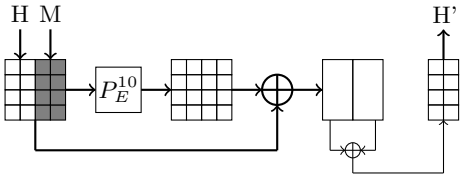

Since ECHO is a nested design of AES-like permutations, we will always use the prefix "BIG" when referring to one of the three layers of the 2048-bit permutation. When not using a prefix, we will refer to the layers of the 2-round AES permutation in the big Sboxes of ECHO.

In the following, $\mathsf{B.SB}_R^{in}$ (respectively $\mathsf{B.SB}_R^{out}$) will denote the whole internal state just before (respectively just after) application of the BIG SubBytes layer during round R (starting the counting from 0). Similarly, $\mathsf{B.MC}_R^{in}$ and $\mathsf{B.MC}_R^{out}$ will stand for the input and output internal states of the BIG MixColumns layer during round R. Of course, we have $\mathsf{B.SB}_R^{in} = \mathsf{B.MC}_{R-1}^{out}$. We refer to [3] for the full specifications.

3.2 Generic differential paths

In order to fully use the power of recent freedom degrees optimization techniques, the core of the differential path we will mainly use will not differ from the ones described in [15,26,27]. The reason here is that this core characteristic is perfectly fit for using the available freedom degrees in the middle: it is computationally very costly in its middle part, but quite cheap on its side parts. This core truncated differential path is 7 rounds long and is depicted in Figure 1. Of course, when attacking a smaller number of rounds than 7, one can use this core to build a further reduced path by cutting off some of the first and/or last rounds.

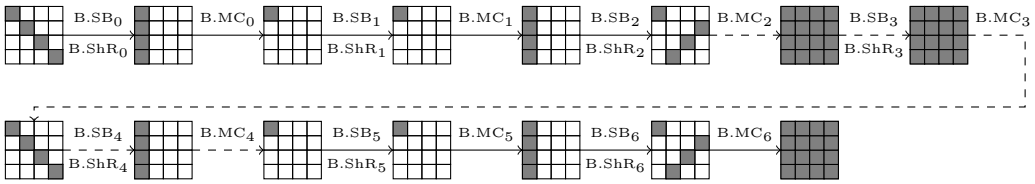

Fig. 1. Core of the truncated differential paths for 7-round reduced ECHO internal permutation. Each cell represents a 128-bit word and a gray cell stands for an active 128-bit word. The controlled rounds are depicted with dashed lines.

One could then use the Super-Sbox technique [15,23] in order to find a pair verifying this differential path. More precisely, one can find a pair of internal states verifying the 128-bit truncated differential trail from the beginning of round 2 ($\mathsf{B.SB}_2^{in}$) up to the end of round 4 ($\mathsf{B.MC}_4^{out}$) with only one operation on average (but with 2^{512} memory and a minimal cost of 2^{512} operations). Note that another view of the attack is to say that with one operation the attacker can find a pair of internal states such that the difference on $\mathsf{B.SB}_2^{out}$ and on $\mathsf{B.MC}_4^{out}$ are chosen (no more truncated differentials). Therefore, for ECHO we consider that the controlled rounds go from $\mathsf{B.SB}_2^{out}$ up to $\mathsf{B.MC}_4^{out}$.

One can easily check that the rest of the path (the uncontrolled rounds) is fulfilled with probability one, except round 1. Indeed, in round 1, a $4 \Rightarrow 1$ truncated differential transition is expected through the backward computation of the BIG MixColumns layer $\mathsf{B.MC}_1$. When dealing with 128-bit truncated differentials, this will happen with approximate probability $2^{-24\times 16} = 2^{-384}$ (i.e. a $4 \Rightarrow 1$ byte-wise truncated differential transition is expected through sixteen parallel $AESMixColumns$ functions). Since one can generate 2^{512} valid candidates for the controlled rounds with 2^{512} computations and memory, the overall complexity is 2^{512} for finding at least one valid pair for the core path from Figure 1. We will see that by looking at byte-wise truncated differentials (instead of word-wise), one can sharpen the differential path and derive an improved Super-Sbox attack for ECHO that requires less memory and minimal number of computations. Also, this allows to improve the success probability of this uncontrolled BIG MixColumns layer. On the other side, in order to be able to use the byte-wise truncated differentials at this stage and since he can control the difference only in $\mathsf{B.SB}_2^{out}$ (and not in $\mathsf{B.SB}_2^{in}$), the attacker will have to handle the backward computation of the BIG SubBytes layer of round 2 ($\mathsf{B.SB}_2$) as well. He then hopes that controlling both $\mathsf{B.SB}_2$ and $\mathsf{B.MC}_1$ with byte-wise truncated differentials will cost less than 2^{384} operations. Not controlling $\mathsf{B.SB}_2$ would lead us back to the 128-bit truncated differential

cryptanalysis, as each active 128-bit word of $\mathsf{B.SB}_2^{in}$ will very likely contain 16 active bytes (i.e. fully active word) since full diffusion is achieved with only two AES rounds.

3.3 Differential transitions for 2 AES rounds

Now that we introduced the core of the differential path, we need to study the word-wise differential transitions. That is, instead of looking for 128-bit truncated differentials, we will look at byte-wise truncated differentials. Of course, we still fully leverage the previous works on Super-Sbox attacks: the attacker can find a valid candidate pair verifying the controlled rounds and fully control the differences in $\mathsf{B.SB}_2^{out}$ and $\mathsf{B.MC}_4^{out}$ with one operation on average. Sharpening the differential path will improve the results since our scope is now wider, but it will also greatly increase the number of potential trails and complicate the analysis. For that reason, we need to heuristically filter them so that we place our search into a good subspace. First, we restrict ourselves to four types of byte-wise truncated differential words F, C, D and 1, all depicted in Figure 2. Secondly, we add the constraint that all the active 128-bit words in an internal state will present the same byte-wise truncated differential (all words have the same truncated differential types F, C, D or 1). This seems a sound constraint as the processing of the BIG MixColumns layer on one word column of the internal state can be seen as the parallel application of sixteen *AESMixColumns* functions (one for each byte position). Thus, for each word column, instead of analyzing the behavior of sixteen parallel *AESMixColumns* functions one conceptually only handles a single function that will do for all the 16. Those two filters will really simplify the analysis.

Fig. 2. Notations for byte-wise truncated differential states for one word of ECHO. Each cell represents a byte and a gray cell stands for an active byte.

Since the attacker will have to control the behavior of BIG SubBytes layer $\mathsf{B.SB}_2$, we have to study the success probability for each possible transition for 2 AES rounds between the four bit-wise truncated differentials F, C, D and 1, especially in backward direction. First, we can compute the approximate probability of success for a one-round transition between those four 128-bit differential states and this is given in Table 2 for both forward and backward directions. Those probabilities are simply obtained by studying the *AESMixColumns* transitions for one AES round (since we are dealing with byte-wise truncated differentials, all the probabilities comes only from the *AESMixColumns* transitions, see [35]).

When computing backward through $\mathsf{B.SB}_2$, the *AESMixColumns* function from the second AES round is the first function to invert. But since this layer is fully linear, one can verify the expected backward transitions by carefully choosing the differences in $\mathsf{B.SB}_2^{out}$ beforehand. Since the Super-Sbox attack allows us such a liberty, the second AES round in $\mathsf{B.SB}_2$ comes for free (one only has to check that the transition is not impossible, i.e. the probability in Table 2 is not null). Finally, having set all the constraints and the cost evaluation, we only have to pick the best backward differential transition through $\mathsf{B.SB}_2$ in terms of probability and active byte weight: $\mathtt{D} \Leftarrow \mathtt{1} \Leftarrow \mathtt{C}$. The transition $\mathtt{D} \Leftarrow \mathtt{1}$ is free as showed by Table 2, while the 2^{-24} probability for the transition $\mathtt{1} \Leftarrow \mathtt{C}$ is not taken in account since we can avoid it by carefully choosing the byte-wise truncated differences in $\mathsf{B.SB}_2^{out}$ beforehand. Therefore, controlling $\mathsf{B.SB}_2$ is now completely free for the attacker.

Now that we controlled the differential behavior of $\mathsf{B.SB}_2$, what is the improvement obtained for the BIG MixColumns layer $\mathsf{B.MC}_1$? Since we only have four active bytes in D, we can focus on controlling 4 parallel *AESMixColumns* transitions instead of 16. We are looking for $4 \Rightarrow 1$ transitions, each

Table 2. Byte-wise truncated differential transition approximated probabilities for one round of AES. The left table shows forward transitions, while the right one gives backward transitions.

Forward				
in \ out	F	C	D	1
F	1	0	2^{-96}	0
C	1	0	0	0
D	0	1	0	2^{-24}
1	0	1	0	0

Backward				
in \ out	F	C	D	1
F	1	2^{-96}	0	0
C	0	0	1	2^{-24}
D	1	0	0	0
1	0	0	1	0

happening with probability 2^{-24}. Thus, for the whole BIG MixColumns layer, we get a probability of $2^{-24\times 4} = 2^{-96}$ and this has to be compared to the previous $2^{-24\times 16} = 2^{-384}$ probability.

3.4 Improved Super-Sbox method for ECHO

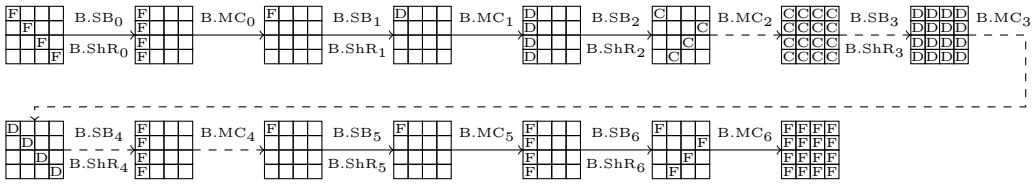

Fig. 3. 7-round differential path for the ECHO internal permutation. The controlled rounds are depicted with dashed lines.

The whole 7-round differential path is depicted in Figure 3 and a valid candidate can be found with complexity 2^{96} operations. However, the Super-Sbox technique still forces us to a minimal complexity of 2^{512} computations and memory. We describe here an improved method that can find a valid candidate for the controlled rounds with minimal cost of 2^{32} computations and memory and with a average cost per solution of 2^{32}. We start by fixing a random column difference for the only active word at the output of $\mathsf{B.MC}_4$ (the very right side of the controlled rounds). One can directly obtain the difference on the output of $\mathsf{B.SB}_4$ by inverting the linear process from the output of $\mathsf{B.MC}_4$. Note that when choosing a random column value at the output of $\mathsf{B.MC}_4$, we do so that when inverting all the linear operations ($\mathsf{B.MC}_4$ and the last MixColumns and ShiftRow layer of $\mathsf{B.SB}_4$) we eventually come to a single active byte in all the four active words (or a single active column in all the four active words) on the output of the second SubBytes layer of $\mathsf{B.SB}_4$. Identically, by fixing random column differences for the four active words at the input of $\mathsf{B.MC}_2$ (the very left side of the controlled rounds), one directly obtains the difference on the input of $\mathsf{B.SB}_3$. Note that as explained previously, this random difference must be chosen so that it fulfills as well the differential transitions $\mathtt{1} \Leftarrow \mathtt{C}$ through the backward computation of the first AES round of $\mathsf{B.SB}_2$. At this point all we have to do is to find a pair of internal state mapping the $\mathsf{B.SB}_3$ input difference to the $\mathsf{B.SB}_4$ output difference. It is easy to check that one can take care of the four 512-bit columns of ECHO independently. Said in other words, we have to handle four independent Super-Sboxes of size 512 bits each. We represent in Figure 4 the situation for a single 512-bit Super-Sbox.

We first do some precomputation work: for the 512-bit column considered, the $\mathsf{B.SB}_3$ layer can be viewed as the parallel application of sixteen 32-bit Super-Sboxes. We already fixed the input differences of those Super-Sboxes and for each one we compute the output difference according to each of the 2^{32}

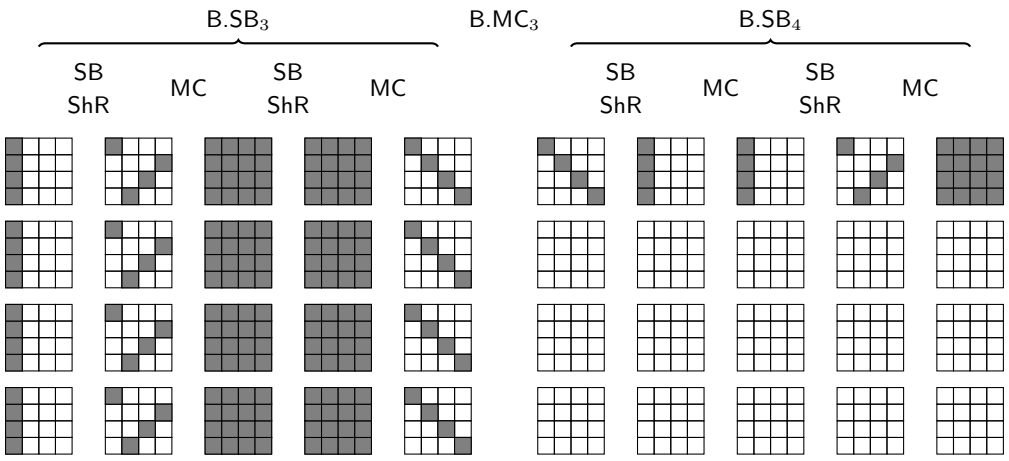

Fig. 4. Improved Super-Sbox technique for ECHO.

possible input values. The output differences are sorted and stored in tables and this step costs us about 2^{32} computations and memory. Later, these tables will allow us to directly find for each Super-Sbox a valid 32-bit candidate value given an output difference.

One can see that in $\mathsf{B.SB}_4$ only a single 32-bit Super-Sbox is active. Moreover, we already fixed the output difference δ of this Super-Sbox. Thus, for each possible 32-bit value v on its output, we compute backward and immediately obtain the corresponding value v' and difference δ' on the input. From δ' we can invert $\mathsf{B.MC}_3$, obtain the output difference on $\mathsf{B.SB}_3$ and we look in the precomputed tables the values mapping to this difference through the sixteen parallel Super-Sboxes of $\mathsf{B.SB}_3$. At this point, it is possible that no candidate exists for each Super-Sbox. However, as described in [15], when a solution is found for each Super-Sbox, we immediately derive several ones by switching the ordering of the pairs. Overall, we can hope for one solution on average.

Once a solution is found for $\mathsf{B.SB}_3$, all differences and values are fixed. However, there is a probability of 2^{-32} that we retrieve the value v' after the forward application of $\mathsf{B.MC}_3$. Thus, by testing all the 2^{32} possible values v, we have a good chance to fulfill this condition and therefore a final solution for the controlled rounds.

Overall, with a minimal cost of 2^{32} computations and memory, one can find a solution for the controlled rounds with 2^{32} computations on average. A valid pair of internal states for the entire differential path from Figure 3 can be obtained with 2^{128} computations and 2^{32} memory.

Since the internal permutation of ECHO is much bigger than its hash output size, it should be easy to distinguish it from a random 2048-bit permutation. Note that our solution pair has four active 128-bit words in the input and four active 128-bit words in the output (the last BIG MixColumns call is not taken in account since it is fully linear). A naive analysis would conclude that for a random 2048-bit permutation, finding such a pair with a birthday paradox technique should require at least $2^{(2048-512)/2} = 2^{768}$ operations. However, since the input and output amount of differences is low, the attacker can not fully leverage the power of the birthday paradox. We conclude by reusing the concept of *limited birthday distinguishers* [15] that for a random 2048-bit permutation, finding such a pair should require at least 2^{1024} operations.[2] Finally, 7 rounds of the internal permutation of ECHO can be distinguished from a random 2048-bit permutation with 2^{128} operations and 2^{32} memory.

The amount of freedom degrees available during the attack is discussed in the Appendix A and a costly distinguisher for 8 rounds of the ECHO internal permutation is given in Appendix B.

[2] The generic attack complexity for mapping through a permutation a fixed difference on i bits on the input and j bits on the output with $i \geq j$ is given by the formula $\max\{2^{j/2}, 2^{i+j-t}\}$, where t is the size of the permutation.

4 Internal differential attack: application to Grøstl

4.1 Description of Grøstl

We give in this section the description of Grøstl and refer to the submission document [14] for more details. Grøstl is a double-pipe hash function that uses a chaining mode similar to the Merkle-Damgård [11, 29] iteration. More precisely, after having initialized the internal state H_0 and padded the input message string, the iteration i updates the $2n$-bit chaining variable H_i with the $2n$-bit incoming message block M_i by applying the compression function h: $H_i = h(H_{i-1}, M_i)$. After having processed all the t message blocks, an output function is applied to the last chaining variable to obtain the n-bit hash result: $hash = trunc_n(P(H_t) \oplus H_t)$, where $trunc_n$ is the truncation function of the n first bits and P is an AES-based permutation. The double-pipe compression function h is built upon two similar parallel AES-based permutations P and Q (that only differ by the constants addition layers) to update chaining variable H with message block M:

$$H' = P(H \oplus M) \oplus Q(M) \oplus H$$

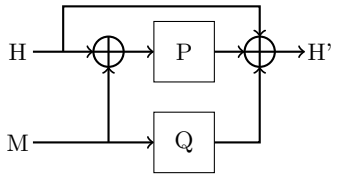

In the case of Grøstl-256, the 512-bit internal state of both permutations can be viewed as a 8×8 matrix of bytes. A byte for permutation P is denoted by $CP_{i,j}$ (resp. $CQ_{i,j}$ for permutation Q), where i is its row position and j its column position in the matrix, starting the counting from 0. P and Q are both 10-round long and each round is composed of 4 layers. The first layer (AddConstant or AC) is a constant addition function. More precisely, for the round number i (starting the counting from 0), in P the byte $CP_{0,0}$ is xored with i and in Q the byte $CQ_{7,0}$ is xored with $i \oplus$ 0xff. **Note that this layer is the only difference between permutations P and Q.** The second layer (SubBytes or SB) is a non-linear function defined by the application of the AES Sbox S to each byte. The third layer (ShiftRows or ShR) cyclically rotates to the left the position of each byte in its own row with the following constants: $(0, 1, 2, 3, 4, 5, 6, 7)$. Finally, the last layer (MixColumns or MC) is a linear function that mixes all the columns of the internal state separately. As for $AESMixColumns$, the matrix multiplication underlying this transformation is a Maximum-Distance Separable mapping. In order to avoid overweighting the notations, we used the same notations for the ECHO and Grøstl subfunctions, but their meaning is implicit depending on which scheme we are dealing with. The round function on an internal state C can thus be defined as:

$$MixColumns \circ ShiftRows \circ SubBytes \circ AddConstant(C).$$

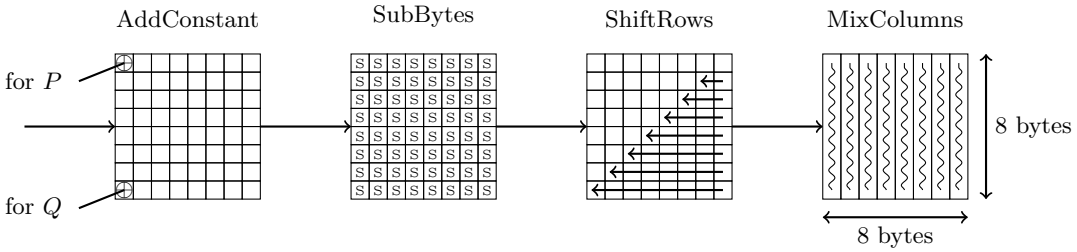

In the case of Grøstl-512, the 1024-bit internal state of both permutations can be viewed as a 8×16 matrix of bytes. P and Q are both 14-round long and each round is composed of the 4 layers. The round function is identical to the Grøstl-256 case, except the rotation constants in the third layer: $(0, 1, 2, 3, 4, 5, 6, 11)$.

4.2 The internal differential attack

In this section, we will show that very good differential trails can be found for Grøstl. Our new technique, ***the internal differential attack***, may apply when a function is built upon parallel computation branches that are not distinct enough. The trick is **to devise a differential path representing the differences between the branches and not between two inputs of the function**. Usually this is avoided by a forcing strong separation between the two parallel branches. For example, for all steps of the hash functions RIPEMD [39] or RIPEMD-160 [12], very distinct constants are used in the left and right branches. However, in the case of Grøstl, this separation is thin between permutations P and Q, and we will describe in the next sections how to exploit this property in order to mount for example a distinguishing attack against the full Grøstl-256 compression function.

All the previous analysis of Grøstl studied the differential behavior of the permutations in a classic way. That is, they derived differential trails by dealing with two different inputs for each of the permutations P and Q (the two permutations were attacked separately). Those permutations mimicking the AES block cipher, the best usable differential paths naturally reached 8 rounds [15], but we argue that much more interesting trails can be built. We do not analyze the two permutations separately, but we build a differential path **between them**: we keep track of the differences ongoing between branch P and branch Q (see Figure 5). We compute two internal states A and B, such that $A \oplus B = \Delta_{IN}$ and such that $P(A) \oplus Q(B) = \Delta_{OUT}$.

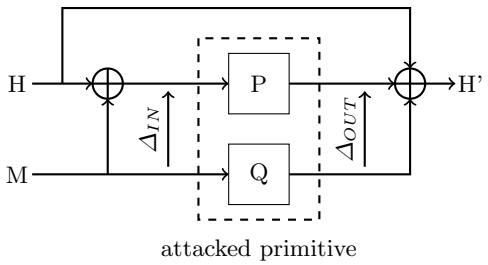

Fig. 5. The differential path keeps track of the differences between permutations P and Q.

This idea comes naturally after having noticed that permutations P and Q are really similar, since their only distinction is the constant addition phase. Even in that step, the distinction is really thin: a different constant is added on only two different bytes. Thus, we can hope that the amount of differences will remain low when setting a differential trail.

Since using truncated differentials is very handy when attacking AES-like permutations, we will only keep track of active and inactive bytes through the path. Also, preparing for the utilization of Super-Sbox attacks, we aim for a differential path in which the costly part lies in the middle, and the cheap parts on the sides. In Figure 16 and 17 from the Appendix D, we provide a differential path between the permutations P and Q of the Grøstl-256 compression function for the 9-round and the 10-round versions respectively. In Figure 18 from the Appendix D, we depict a differential path between the permutations P and Q of the Grøstl-512 compression function reduced to 11 rounds. Note that only one difference is incorporated during AC_0 since the constant added in P is 0.

4.3 Deriving a distinguisher for the Grøstl compression function or internal permutations

In the following, our goal is to distinguish the Grøstl compression function from an ideal primitive on the same domain. As shown in Figure 5, once the differential path settled, we find a valid pair of internal states (A, B) such that

$$A \oplus B = \Delta_{IN}$$
$$P(A) \oplus Q(B) = \Delta_{OUT}$$

where Δ_{IN} and Δ_{OUT} are respectively the input and output truncated differences. We then set $H = A \oplus B$ and $M = B$ and we obtain

$$h(H, M) = P(A) \oplus Q(B) \oplus A \oplus B = \Delta_{IN} \oplus \Delta_{OUT}.$$

We will show that Δ_{IN} and Δ_{OUT} are always maintained in a small subspace of x and y elements respectively. As a consequence, $\Delta_{IN} \oplus \Delta_{OUT}$ will also belong to a small subspace of the full output domain. Said in other words, we will be able to compute outputs of the $2n$-bit compression function that always belong to a predetermined set of at most $k = x \cdot y$ elements. In the ideal case, one such input/output property should not be obtained with substantially less than $2^{2n}/k$ compression function calls. Unlike the previously known distinguishers that find partially colliding outputs for AES-like permutations, the one we describe here is more "preimage" oriented.

One can go further and even try to distinguish the Grøstl compression function from its internal construction

$$h(H, M) = P(H \oplus M) \oplus Q(M) \oplus H = (P(A) \oplus A) \oplus (Q(B) \oplus B)$$

assuming P and Q as ideal permutations. We will compute pairs (H, M) such that H belong to a small subspace of x elements and H' to a small subspace of $k = x \cdot y$ elements. In the ideal case, one may think that the best attack can obtain such a property this with $\min\{\sqrt{2^{2n}/x}, \sqrt{2^{2n}/y}\}$ computations by performing a birthday method with the two branches. However, this is not the case here because a strong constraint exists on the amount of differences between the two branches on the input and the output (see the limited birthday distinguishers [15]) and the best known complexity to obtain the input/output property with ideal permutations P and Q is $2^{2n}/(k \cdot x)$ computations. It is important to remark that this type of distinguisher is new since the already known ones are structural, i.e. they already consider P and Q as ideal permutations.

Even simpler, one can distinguish the construction $f(a, b) = P(a) \oplus Q(b)$ when P and Q are ideal permutations or the Grøstl internal permutations. The value of $a \oplus b$ is maintained in a subspace of x elements and the output is maintained in a subspace of y elements. The limited birthday distinguisher [15] implies that $2^{2n}/k$ computations are required to find such a candidate in the ideal permutations case. This will show that permutations P and Q are not ideal.

While formally defining a distinguisher for a keyless primitive is difficult [40], we argue that the property we exhibit here works for any choice of Sbox, MixColumns function or AddConstant positions for example. Note that such keyless primitive distinguishers have already been utilized in [15, 26].

Let Grøstl(a) denote the Grøstl hash function for which the constant addition in Q is $i \oplus a$ instead of $i \oplus$ 0xff. Clearly, when choosing $a >$ 0x1a, we ensure that the constant values added in P and Q are always distinct and each member of this family of Grøstl hash functions should have the same security as Grøstl(0xff). Overall, for each member of the family, the attacker can exhibit with good probability an output maintained in the set of k elements, while the input H belongs to the subspace of x elements. Thus, if we are queried to distinguish the Grøstl compression function instantiated with permutations corresponding to Grøstl(a) from the same construction with random permutations P and Q, we have a very good probability to succeed. It shows a weakness in the Grøstl design philosophy.

4.4 Finding a collision for the hash function

One can use the internal differential attack in order to find a collision for the reduced Grøstl hash function. Note that this is usually much harder than finding a collision for the compression function only. We provide in Figure 6 a differential path for 5 rounds of Grøstl-256. Note that the very first state is fully active and can be forced to any random difference value since located in the controlled rounds.

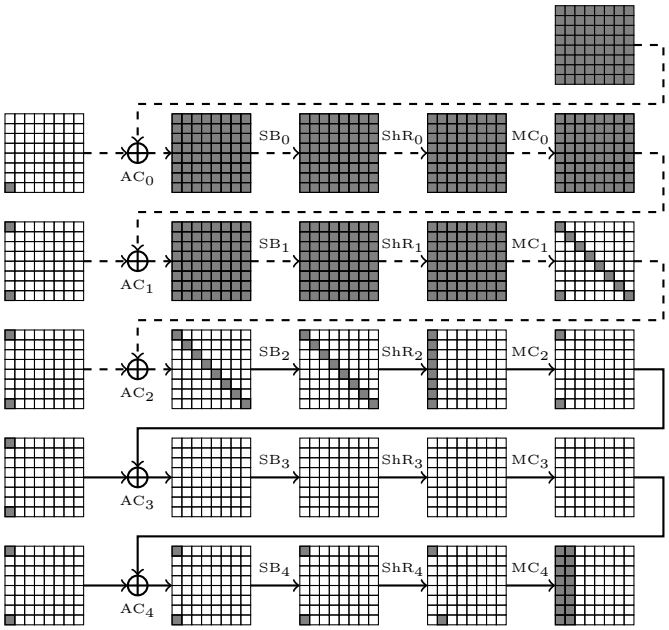

Fig. 6. 5-round differential path between P and Q for Grøstl-256. Each cell represents a byte and a gray cell stands for an active byte. The controlled rounds are depicted with dashed lines. The matrices on the left represent the differences incorporated during the AC layers.

The idea of the attack is the following: by choosing a random message prefix Pre, we obtain a random chaining variable value that we denote R and we have $\Delta_{IN} = R$. Then, we find two valid message block candidates M_1 and M_2 for the differential path starting from R. We denote by Δ^1_{OUT} and Δ^2_{OUT} their respective output differences. We have

$$h(R, M_1) = R \oplus \Delta^1_{OUT} \text{ and } h(R, M_2) = R \oplus \Delta^2_{OUT}.$$

Thus, if $\Delta^1_{OUT} = \Delta^2_{OUT}$, then $h(R, M_1) = h(R, M_2)$ and $(Pre||M_1, Pre||M_2)$ is a colliding message pair for the hash function. Note that in this scenario, we have largely enough freedom degree in order to find the collision since we can choose a large set of message prefix.

5 Results

In this section we present our results on the compression functions of ECHO and Grøstl. For completeness, we give in the Appendix C the analysis for the single-pipe version ECHO-SP. Moreover, we also provide in the Appendix A a study of the amount of freedom degrees available during the attacks.

5.1 Distinguishers for the ECHO compression function

ECHO-256. We use the 4-round differential path from Figure 7 which is derived from the 7-round core path. The uncontrolled part requires 2^{64} candidates (through the backward computation of $\mathsf{B.MC}_0$), while the improved Super-Sbox method for ECHO generates one valid candidate for the controlled part with 2^{32} computations and 2^{32} memory. Overall, we obtain a valid pair for the whole differential path with 2^{96} computations and 2^{32} memory (2^{32} such pairs can be generated by the attacker and 2^{160} if the salt is controlled as well).

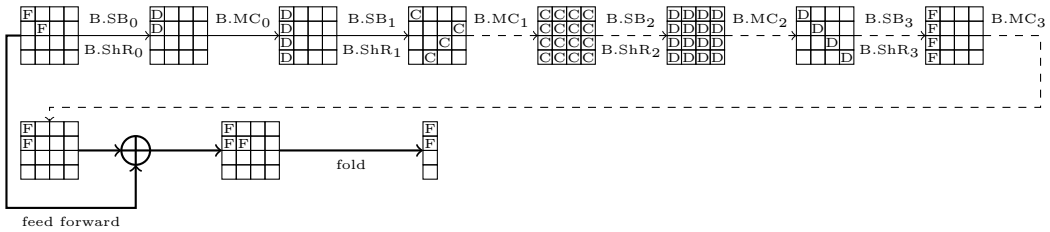

Fig. 7. 4-round differential path for the ECHO-256 compression function distinguisher. The controlled rounds are depicted with dashed lines.

ECHO-512. We use the 6-round differential path from Figure 8 also derived from the 7-round core path. The uncontrolled part requires 2^{64} candidates (through the backward computation of $\mathsf{B.MC}_1$), while the improved Super-Sbox method for ECHO generates one valid candidate for the controlled part with 2^{32} computations and 2^{32} memory. Overall, we obtain a valid pair for the whole differential path with 2^{96} computations and 2^{32} memory (2^{32} such pairs can be generated by the attacker and 2^{160} if the salt is controlled as well).

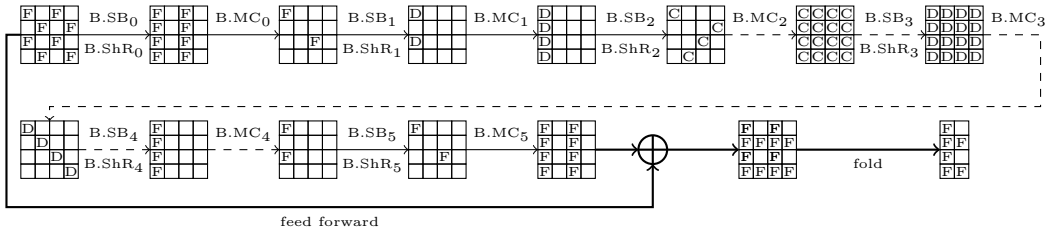

Fig. 8. 6-round differential path for the ECHO-512 compression function distinguisher. The controlled rounds are depicted with dashed lines.

In both cases, we obtain compression function outputs colliding on 2 predetermined words (i.e. 256 bits) and this should require 2^{128} computations in the ideal case. Note that since all active 128-bit words in the end of the differential path are fully active, we could have added another B.SB layer and attacked one more half-round.

5.2 Collisions for the ECHO compression function

ECHO-256. We use a special 3-round differential path depicted in Figure 9. In this trail, the improved Super-Sbox technique for ECHO can be applied exactly as previously explained for the 7-round core path. Thus, a valid candidate for the controlled rounds can be found with 2^{32} computations and 2^{32} memory, while the uncontrolled part is verified with probability 1. Note that the column differences after $\mathsf{B.MC}_2$ can be chosen beforehand so that they xor to zero during the folding phase. Using the freedom degrees counting method, one can check that only 2^{32} valid pair can be obtained with this extra condition. However, in order to get a collision on the output, we have to make the diagonal differences on the input collide during the folding phase. Since we have 32 bit positions concerned, the attacker has to go through those 2^{32} candidates and finally the attack complexity is 2^{64} computations and 2^{32} memory in order to find a free-start collision attack for the ECHO-256 compression function.

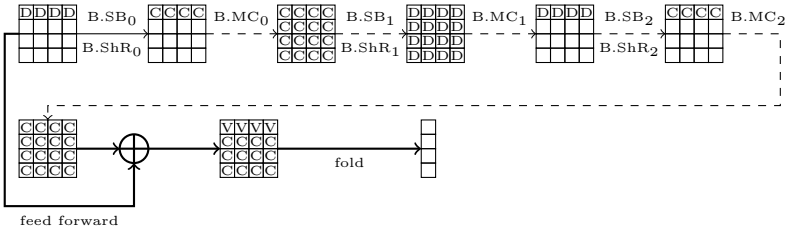

Fig. 9. 3-round differential path for the ECHO-256 compression function free-start collision attack. The controlled rounds are depicted with dashed lines. We denote by V an AES word with one column and one diagonal active.

Similarly, a chosen-salt semi-free-start collision attack could be obtained by using the differential path from Figure 10. The situation is exactly the same as previously, except that one has 64 bit positions to collide on and the salt will have to be randomized on 2^{32} values in order to provide enough freedom degrees. Thus, finding a chosen-salt semi-free-start collision attack for the ECHO-256 compression function requires 2^{96} computations and 2^{32} memory.

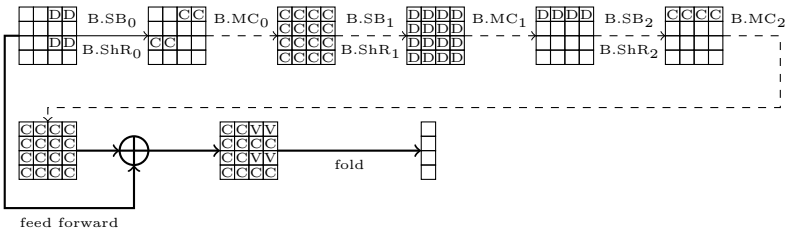

Fig. 10. 3-round differential path for the ECHO-256 compression function chosen-salt semi-free-start collision attack. The controlled rounds are depicted with dashed lines. We denote by V an AES word with one column and one diagonal active.

ECHO-512. We use the 3-round differential path depicted in Figure 11. The situation is exactly the same as for the path from Figure 10. Therefore, one can derive a chosen-salt semi-free-start collision attack for the ECHO-512 compression function with 2^{96} computations and 2^{32} memory.

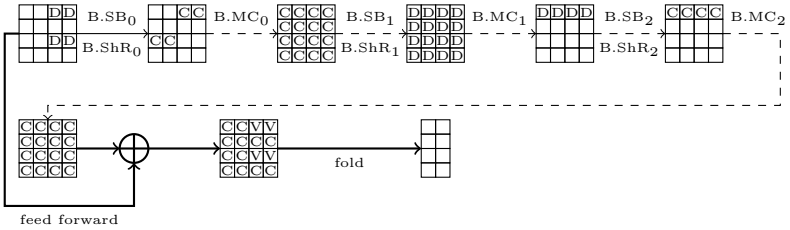

Fig. 11. 3-round differential path for the ECHO-512 compression function chosen-salt (semi)-free-start collision attack. The controlled rounds are depicted with dashed lines. We denote by V an AES word with one column and one diagonal active.

5.3 Distinguishers for the Grøstl compression function

Grøstl-256. We use the Super-Sbox technique to find two 512-bit internal states such that the 9-round differential path from Figure 16 between permutations P and Q is verified. Namely, one can find internal state values for P and Q verifying the truncated differential trail from the output of SB_2 up to the input of SB_5 with one computation on average. However, the $8 \mapsto 2$ MixColumns transition through MC_5 during the uncontrolled rounds is verified with probability 2^{-48}. Also, 2 byte differences must be erased during both AddConstant functions AC_2 and AC_6 which adds another $2^{-4\times 8} = 2^{-32}$ factor. Overall, one can find a valid candidate for the whole path with only $2^{48+32} = 2^{80}$ computations (an amount of 2^{64} memory is required by the Super-Sbox technique).

Regarding the 10-round differential path from Figure 17, the controlled rounds go from the output of SB_3 up to the input of SB_6. Then, the two $8 \mapsto 1$ MixColumns transitions through MC_2 and the $8 \mapsto 2$ transition through MC_6 during the uncontrolled rounds happen with probability $2^{-2\times 56} = 2^{-112}$ and 2^{-48} respectively. Also, 2 byte differences must be erased during both AddConstant functions AC_2 and AC_7 which adds another $2^{-4\times 8} = 2^{-32}$ factor. Overall, one can find a valid candidate for the whole path with only $2^{112+48+32} = 2^{192}$ computations (again, an amount of 2^{64} memory is required by the utilization of the Super-Sbox technique).

The freedom degrees analysis from Appendix A shows that for both paths from Figure 16 and 17, one can expect to obtain one solution with good probability. Indeed, for both paths, when the success probability for a random input pair to verify the trail is 2^{-z}, we have about 2^z freedom degrees available. We argue in the Appendix that it is sufficient for the attack to be considered as valid and we give in Section 5.5 a method that provides some additional freedom degrees.

Grøstl-512. As for Grøstl-256, we use the Super-Sbox technique to find two 1024-bit internal states such that the 11-round differential path from Figure 18 between permutations P and Q is verified. Namely, one can find internal state values for P and Q from the output of SB_3 up to the input of SB_6 with one computation on average. However, the MixColumns transition through MC_6 during the uncontrolled rounds happens with probability $2^{-(48+7\times 56)} = 2^{-440}$: the first column is a $8 \mapsto 2$ transition, while the second, third, fourth, fifth, sixth, seventh and twelfth are $8 \mapsto 1$ transitions. The next MixColumns layer MC_7 contains a $8 \mapsto 2$ transition, adding another factor 2^{-48}. Regarding MC_2, the first and sixth columns are $8 \mapsto 1$ transitions, thus successfully verified with a total probability of $2^{-2\times 56} = 2^{-112}$.

Also, 2, 1 and 2 byte differences must be erased during AddConstant functions AC_2, AC_7 and AC_8 respectively. This adds another $2^{-5\times 8} = 2^{-40}$ factor. Overall, one can find a valid candidate for the whole path with $2^{440+48+112+40} = 2^{640}$ computations (an amount of 2^{64} memory is required by the Super-Sbox technique for `Grøstl`). Again, the freedom degrees analysis shows that we can expect one solution with good probability.

The distinguisher for `Grøstl` compression function and internal permutations. In order to mount the distinguisher for `Grøstl`, one has to analyze the amount k of reachable output difference values. The situation is completely identical for the paths from Figures 16 and 17 in the Appendix, but we will use the notations from the second one. We have 16 active bytes just before applying the very last MixColumns layer MC_9. Since the MixColumns layer is fully linear, the amounts of reachable difference values on its input and on its output are equal. Thus, we can deduce that at most $y = 2^{16\times 8} = 2^{128}$ distinct output differences can be reached on the output of the differential trail. Regarding the input of the path, the same reasoning gives us that at most $x = 2^{8\times 8} = 2^{64}$ distinct input differences can be reached. Note that the difference inserted during AC_0 can be ignored since it is the last layer when computing backward (the difference value on that byte will always be equal to the constant added, i.e. `0xff`). Also, it is easy to verify that the differences on the output of SB_0 are always the same (since MixColumns is linear). Thus, since the inverse of the `AES` Sbox has the property that only 2^7 distinct output differences can be reached when the input difference is fixed, we can conclude that Δ_{IN} can go through a maximum of $x = 2^{8\times 7} = 2^{56}$ distinct values.

To summarize, the output chaining variable $H' = h(H, M) = \Delta_{IN} \oplus \Delta_{OUT}$ is limited to a set of at most $k = 2^{128+56} = 2^{184}$ values, with H being limited to a set of at most $x = 2^{56}$ values. For an ideal 512-bit compression function, reaching any element of this set should require $2^{512-184} = 2^{328}$ operations. With 2^{80} and 2^{192} computations respectively (and 2^{64} memory), we finally conclude that our attack can distinguish 9-round reduced or the full 10-round compression function of `Grøstl`-256 from a random 512-bit compression function. One can even distinguish h from the compression function construction with P and Q assumed ideal since the best known attack requires $2^{512-184-56} = 2^{272}$ computations. Moreover, the ideal case complexity to find such a candidate for the $f(a, b) = P(a) \oplus Q(b)$ construction is $2^{512-184} = 2^{328}$ operations and this shows that permutations P and Q can not be considered ideal functions.

In the case of `Grøstl`-512 (see Figure 18 in the Appendix D), the same reasoning tells us that Δ_{IN} can go through a maximum of $x = 2^{56}$ values and Δ_{OUT} through a maximum of $y = 2^{128}$ values. Thus, the output chaining variable $H' = h(H, M) = \Delta_{IN} \oplus \Delta_{OUT}$ is limited to a set of at most $k = 2^{128+56} = 2^{184}$ values, with H being limited to a set of at most $x = 2^{56}$ values. For an ideal 1024-bit compression function, reaching any element of this set should require $2^{1024-184} = 2^{840}$ operations. We conclude that our 2^{640} computations (and 2^{64} memory) attack can distinguish a 11-round reduced version of the `Grøstl`-512 compression function from a random 1024-bit compression function. Again, one can even distinguish h from the compression function construction with P and Q assumed ideal since the best known attack requires $2^{1024-184-56} = 2^{784}$ computations. Also, the ideal case complexity to find such a candidate for the $f(a, b) = P(a) \oplus Q(b)$ construction is $2^{1024-184} = 2^{840}$ operations.

Note that structural distinguishers (i.e. working for randomly chosen permutations P and Q) already exist for `Grøstl`. For example, just like in the Davies-Meyer construction, one can very easily find fixed points for the compression function. Yet, as explained in Section 4.3, we believe that our distinguishers are very interesting because they exploit the real differential properties of the internal permutations P and Q, which is essential in order to appropriately evaluate the security margin in terms of number of rounds. Moreover, such structural attacks can not distinguish h from the compression function construction with P and Q assumed ideal. Finally, we showed that full permutations P and Q for the 256-bit case can not be considered as ideal permutations.

5.4 Collisions for the `Grøstl` hash function

`Grøstl`-256. We use the differential path from Figure 6. One can check that the output difference comes from the AC_5 layer that adds two fixed byte differences. On the output of the next SubBytes layer, this

leads to 2^{14} distinct reachable difference values (this amount is not modified after the application of the last linear MC layer). Thus, with two valid candidates M_1 and M_2, we have a probability 2^{-14} that they will match on their output difference.

Now, we have to compute the complexity for finding one single candidate for the trail. The classical application of the Super-Sbox technique gives us an average cost of one operation per solution for the controlled rounds, with a minimal cost of 2^{64} computations and memory. The uncontrolled rounds are verified with probability 2^{-64} (2^{-48} for MC_3 and 2^{-16} for AC_4). Thus a colliding pair of messages for the Grøstl-256 hash function reduced to 5 rounds can be found with $2^{64+14+1} = 2^{79}$ computations and 2^{64} memory.

Grøstl-512. We use the 6-round differential path from Figure 19 in the Appendix D. One can check that the output difference comes from the AC_5 and AC_6 layers that adds fixed byte differences. After the application of AC_6, we have 16 active bytes, which leads to $2^{16*7} = 2^{112}$ distinct reachable difference values after the next SubBytes layer (this amount is not modified after the application of the last linear MC layer). Thus, with two valid candidates M_1 and M_2, we have a probability 2^{-112} that they will match on their output difference.

Now, we have to compute the complexity for finding one single candidate for the trail. The classical application of the Super-Sbox technique gives us an average cost of one operation per solution for the controlled rounds, with a minimal cost of 2^{64} computations and memory. The uncontrolled rounds are verified with probability 2^{-64} (2^{-48} for MC_3 and 2^{-16} for AC_4). Thus a colliding pair of messages for the Grøstl-512 hash function reduced to 6 rounds can be found with $2^{64+112+1} = 2^{177}$ computations and 2^{64} memory.

5.5 Generalizing the internal differential attack

One can further generalize the internal differential attack in order to obtain more freedom degrees. We previously looked at the differences between permutations P and Q at the very same byte positions, i.e. we looked a the difference between $CP_{i,j}$ and $CQ_{i,j}$. However, an observation on AES-like permutation symmetries allows us to do else: if one only considers functions SB, ShR and MC, an input composed of columns with the same value will always maintain this property though the round process. In general, this symmetry issue is avoided with the key addition, or the AC layer in Grøstl. In the internal differential attack, this layer is already directly composing our differential path, so we can leverage this property.

More precisely, we will now look at the differences between $CP_{i,j}$ and $CQ_{i,(j+r) \bmod c}$, where c is the number of columns of the AES-like state (8 for Grøstl-256 and 16 for Grøstl-512) and $0 \leq r < c$ is a fixed parameter. Said in other words, we look at the difference between P and a column-rotated variant of Q. One can easily check that this is not going to change anything to our differential paths in regards to SB, ShR and MC because of this column symmetry consideration. However, during the AC layer, the column position of the constant additions in Q will "virtually" change. For example, in the case of Grøstl-256, if $r = 1$ the only effect on the differential path between P and Q will be that the addition of the constant in Q will move to the last column in each round.

Therefore, one can see that we will deal with 8 or 16 distinct differential paths DP_r, discriminated only by the parameter r that changes the virtual column position of the constant addition in Q. For example, in the previous sections or in Figure 16 and 17 from the Appendix D, we used only DP_0 since we had $r = 0$.

We explained in Section 5.3 that a valid candidate for the 10-round variant of the differential path DP_0 for Grøstl-256 can be found with 2^{192} computations and 2^{64} memory (or 2^{80} computations and 2^{64} memory for the 9-round variant), and this will also be the case of DP_1. However, the six other DP_r have one additional active column in the uncontrolled rounds, and an additional 2^{64} complexity factor is required. Moreover, the input/output subspaces are also different depending on the value of r and this is summarized in Table 3, together with the Grøstl-512 case.

Note that each differential path DP_r will have the same probability that a solution can be found. This offers a chance to the attacker to perform the attack again in case a solution could not be found for

Table 3. Extending the internal differential attack for Grøstl. Depending on the differential path considered, and the class DP_r considered, we provide the complexity required in order to find a valid candidate, as well as the input/output subspaces sizes in which the candidate is contained. The last column shows the complexity to find such a candidate for the $f(a,b) = P(a) \oplus Q(b)$ construction in the ideal case ($2^{2n}/k$).

	differential path	differential path class	time/memory complexity	subspace size input	subspace size output	internal permutations ideal case complexity
Grøstl-256	9 rounds, Fig. 16	DP_0	$2^{80}/2^{64}$	2^{56}	2^{128}	2^{328}
		DP_1	$2^{144}/2^{64}$	2^{112}	2^{64}	2^{336}
		DP_r, $r \geq 2$	$2^{144}/2^{64}$	2^{112}	2^{128}	2^{272}
	10 rounds, Fig. 17	DP_0	$2^{192}/2^{64}$	2^{56}	2^{128}	2^{328}
		DP_1	$2^{192}/2^{64}$	2^{112}	2^{64}	2^{336}
		DP_r, $r \geq 2$	$2^{256}/2^{64}$	2^{112}	2^{128}	2^{272}
Grøstl-512	11 rounds, Fig. 18	DP_0	$2^{640}/2^{64}$	2^{56}	2^{128}	2^{840}
		DP_1	$2^{768}/2^{64}$	2^{112}	2^{128}	2^{784}
		DP_2	$2^{832}/2^{64}$	2^{112}	2^{128}	2^{784}
		DP_3	$2^{896}/2^{64}$	2^{112}	2^{128}	2^{784}
		DP_4	$2^{960}/2^{64}$	2^{112}	2^{128}	2^{784}
		DP_5	$2^{832}/2^{64}$	2^{112}	2^{64}	2^{848}
		DP_6	$2^{960}/2^{64}$	2^{112}	2^{128}	2^{784}
		DP_7	$2^{1024}/2^{64}$	2^{112}	2^{128}	2^{784}
		DP_8	$2^{1024}/2^{64}$	2^{112}	2^{128}	2^{784}
		DP_9	$2^{1024}/2^{64}$	2^{112}	2^{128}	2^{784}
		DP_{10}	$2^{960}/2^{64}$	2^{112}	2^{128}	2^{784}
		DP_{11}	$2^{896}/2^{64}$	2^{112}	2^{128}	2^{784}
		DP_{12}	$2^{960}/2^{64}$	2^{112}	2^{128}	2^{784}
		DP_{13}	$2^{896}/2^{64}$	2^{112}	2^{128}	2^{784}
		DP_{14}	$2^{832}/2^{64}$	2^{112}	2^{128}	2^{784}
		DP_{15}	$2^{768}/2^{64}$	2^{112}	2^{128}	2^{784}

a DP_r. However, this will only help in the case we are trying to distinguish the permutations P and Q from ideal permutations. Indeed, in the situation of a compression function distinguisher, the subspace properties we will observe on the output when $k \neq 0$ are too restricted.

6 Conclusion

In this article, based on recent advances on AES-like permutations studies, we provided a new cryptanalysis of ECHO and Grøstl, two second-round SHA-3 candidates. In particular, in the case of Grøstl, we introduce a new cryptanalysis technique: the internal differential attack. Overall, we obtain the best cryptanalysis results known so far for both ECHO and Grøstl. We are able to derive a distinguisher for the full (10 rounds) 256-bit version of the Grøstl compression function or internal permutations. This work also shows that designers must be careful when building a function with parallel branches computations as the internal differential paths may lead to unexpected attacks.

Acknowledgments

The author would like to thank the Grøstl team, Henri Gilbert, Yannick Seurin and the CRYPTO 2010 committee for their helpful comments. Also, many thanks to Elmar Tischhauser, Jorge Nakahara and Kota Ideguchi for pointing me an omission in the complexity computation for the full ECHO internal permutation distinguisher and the inconsistency in the direct utilization of the start-from-the-middle attack for ECHO in [26].

References

1. P.S.L.M. Barreto. An observation on Grøstl. Comment submitted to the NIST hash function mailing list, hash-forum@nist.gov. http://www.larc.usp.br/~pbarreto/Grizzly.pdf.
2. Mihir Bellare and Phillip Rogaway. Random Oracles are Practical: A Paradigm for Designing Efficient Protocols. In *ACM Conference on Computer and Communications Security*, pages 62–73, 1993.
3. Ryad Benadjila, Olivier Billet, Henri Gilbert, Gilles Macario-Rat, Thomas Peyrin, Matt Robshaw, and Yannick Seurin. SHA-3 Proposal: ECHO. Submission to NIST, 2008. Available online at http://crypto.rd.francetelecom.com/echo/.
4. Eli Biham and Orr Dunkelman. A Framework for Iterative Hash Functions: HAIFA. Second NIST Cryptographic Hash Workshop, 2006.
5. Eli Biham and Orr Dunkelman. The SHAvite-3 Hash Function. Submission to NIST, 2008.
6. Alex Biryukov, editor. *Fast Software Encryption, 14th International Workshop, FSE 2007, Luxembourg, Luxembourg, March 26-28, 2007, Revised Selected Papers*, volume 4593 of *Lecture Notes in Computer Science*. Springer, 2007.
7. Alex Biryukov, Dmitry Khovratovich, and Ivica Nikolic. Distinguisher and Related-Key Attack on the Full AES-256. In Halevi [16], pages 231–249.
8. Gilles Brassard, editor. *Advances in Cryptology - CRYPTO '89, 9th Annual International Cryptology Conference, Santa Barbara, California, USA, August 20-24, 1989, Proceedings*, volume 435 of *Lecture Notes in Computer Science*. Springer, 1990.
9. Ronald Cramer, editor. *Advances in Cryptology - EUROCRYPT 2005, 24th Annual International Conference on the Theory and Applications of Cryptographic Techniques, Aarhus, Denmark, May 22-26, 2005, Proceedings*, volume 3494 of *Lecture Notes in Computer Science*. Springer, 2005.
10. Joan Daemen and Vincent Rijmen. *The Design of Rijndael*. Information Security and Cryptography. Springer, 2002. ISBN 3-540-42580-2.
11. Ivan Damgård. A Design Principle for Hash Functions. In Brassard [8], pages 416–427.
12. H. Dobbertin, A. Bosselaers, and B. Preneel. RIPEMD-160: A Strengthened Version of RIPEMD. In D. Gollmann, editor, Fast Software Encryption – FSE 96, volume 1039 of *Lecture Notes in Computer Science*, pages 71–82. Springer, 1996.
13. Orr Dunkelman, editor. *Fast Software Encryption, 16th International Workshop, FSE 2009, Leuven, Belgium, February 22-25, 2009, Revised Selected Papers*, volume 5665 of *Lecture Notes in Computer Science*. Springer, 2009.
14. Praveen Gauravaram, Lars R. Knudsen, Krystian Matusiewicz, Florian Mendel, Christian Rechberger, Martin Schläffer, and Søren S. Thomsen. Grøstl – a SHA-3 candidate. Submission to NIST, 2008. Available online at http://www.groestl.info.
15. Henri Gilbert and Thomas Peyrin. Super-Sbox Cryptanalysis: Improved Attacks for AES-like Permutations. In Fast Software Encryption – FSE 2010, volume 6147 of *Lecture Notes in Computer Science*, pages 365–383. Springer, 2010. Available online at http://eprint.iacr.org/2009/531.
16. Shai Halevi, editor. *Advances in Cryptology - CRYPTO 2009, 29th Annual International Cryptology Conference, Santa Barbara, CA, USA, August 16-20, 2009. Proceedings*, volume 5677 of *Lecture Notes in Computer Science*. Springer, 2009.
17. Michael J. Jacobson Jr., Vincent Rijmen, and Reihaneh Safavi-Naini, editors. *Selected Areas in Cryptography, 16th Annual International Workshop, SAC 2009, Calgary, Alberta, Canada, August 13-14, 2009, Revised Selected Papers*, volume 5867 of *Lecture Notes in Computer Science*. Springer, 2009.
18. J. Kelsey. Some notes on Grøstl. Comment submitted to the NIST hash function mailing list, hash-forum@nist.gov. http://ehash.iaik.tugraz.at/uploads/d/d0/Grostl-comment-april28.pdf.
19. Dmitry Khovratovich. Cryptanalysis of Hash Functions with Structures. In Jacobson Jr. et al. [17], pages 108–125.

20. Lars R. Knudsen, Christian Rechberger, and Søren S. Thomsen. The Grindahl Hash Functions. In Biryukov [6], pages 39–57.
21. Lars R. Knudsen and Vincent Rijmen. Known-Key Distinguishers for Some Block Ciphers. In K. Kurosawa, editor, *ASIACRYPT*, volume 4833 of *Lecture Notes in Computer Science*, pages 315–324. Springer, 2007.
22. L.R. Knudsen. Truncated and Higher Order Differentials. In B. Preneel, editor, Fast Software Encryption – FSE 1994, volume 1008 of *Lecture Notes in Computer Science*, pages 196–211. Springer, 1994.
23. Mario Lamberger, Florian Mendel, Christian Rechberger, Vincent Rijmen, and Martin Schläffer. Rebound Distinguishers: Results on the Full Whirlpool Compression Function. In Matsui [24], pages 126–143.
24. Mitsuru Matsui, editor. *Advances in Cryptology - ASIACRYPT 2009, 15th International Conference on the Theory and Application of Cryptology and Information Security, Tokyo, Japan, December 6-10, 2009. Proceedings*, volume 5912 of *Lecture Notes in Computer Science*. Springer, 2009.
25. Krystian Matusiewicz, María Naya-Plasencia, Ivica Nikolic, Yu Sasaki, and Martin Schläffer. Rebound Attack on the Full Lane Compression Function. In Matsui [24], pages 106–125.
26. Florian Mendel, Thomas Peyrin, Christian Rechberger, and Martin Schläffer. Improved Cryptanalysis of the Reduced Grøstl Compression Function, ECHO Permutation and AES Block Cipher. In Jacobson Jr. et al. [17], pages 16–35.
27. Florian Mendel, Christian Rechberger, Martin Schläffer, and Søren S. Thomsen. The Rebound Attack: Cryptanalysis of Reduced Whirlpool and Grøstl. In Dunkelman [13], pages 260–276.
28. Florian Mendel, Christian Rechberger, Martin Schläffer, and Søren S. Thomsen. Rebound Attacks on the Reduced Grøstl Hash Function. In Pieprzyk [37], pages 350–365.
29. Ralph C. Merkle. One Way Hash Functions and DES. In Brassard [8], pages 428–446.
30. Marine Minier, Raphael C.-W. Phan, and Benjamin Pousse. Distinguishers for Ciphers and Known Key Attack against Rijndael with Large Blocks. In Preneel [38], pages 60–76.
31. National Institute of Standards and Technology. FIPS 180-1: Secure Hash Standard. `http://csrc.nist.gov`, April 1995.
32. National Institute of Standards and Technology. FIPS PUB 197, Advanced Encryption Standard (AES). Federal Information Processing Standards Publication 197, U.S. Department of Commerce, November 2001.
33. National Institute of Standards and Technology. Announcing Request for Candidate Algorithm Nominations for a New Cryptographic Hash Algorithm (SHA-3) Family. *Federal Register*, 27(212):62212–62220, November 2007. Available:`http://csrc.nist.gov/groups/ST/hash/documents/FR_Notice_Nov07.pdf`(2008/10/17).
34. Phong Q. Nguyen, editor. *Progressin Cryptology - VIETCRYPT 2006, First International Conferenceon Cryptology in Vietnam, Hanoi, Vietnam, September 25-28, 2006, Revised Selected Papers*, volume 4341 of *Lecture Notes in Computer Science*. Springer, 2006.
35. Thomas Peyrin. Cryptanalysis of Grindahl. In Kaoru Kurosawa, editor, *ASIACRYPT*, volume 4833 of *Lecture Notes in Computer Science*, pages 551–567. Springer, 2007.
36. Thomas Peyrin. Improved Differential Attacks for ECHO and Grostl. Cryptology ePrint Archive, Report 2010/223, 2010. `http://eprint.iacr.org/`.
37. Josef Pieprzyk, editor. *Topics in Cryptology - CT-RSA 2010, The Cryptographers' Track at the RSA Conference 2010, San Francisco, CA, USA, March 1-5, 2010. Proceedings*, volume 5985 of *Lecture Notes in Computer Science*. Springer, 2010.
38. Bart Preneel, editor. *Progress in Cryptology - AFRICACRYPT 2009, Second International Conference on Cryptology in Africa, Gammarth, Tunisia, June 21-25, 2009. Proceedings*, volume 5580 of *Lecture Notes in Computer Science*. Springer, 2009.
39. RIPE. Integrity Primitives for Secure Information Systems. In A. Bosselaers and B. Preneel, editors, *Final Report of RACE Integrity Primitives Evaluation (RIPE-RACE 1040)*, volume 1007 of *Lecture Notes in Computer Science*. Springer, 1995.
40. Phillip Rogaway. Formalizing Human Ignorance. In Nguyen [34], pages 211–228.
41. Ronald L. Rivest. RFC 1321: The MD5 Message-Digest Algorithm. `http://www.ietf.org/rfc/rfc1321.txt`, April 1992.
42. Victor Shoup, editor. *Advances in Cryptology - CRYPTO 2005: 25th Annual International Cryptology Conference, Santa Barbara, California, USA, August 14-18, 2005, Proceedings*, volume 3621 of *Lecture Notes in Computer Science*. Springer, 2005.
43. David Wagner. A Generalized Birthday Problem. In Yung [46], pages 288–303.
44. Xiaoyun Wang, Yiqun Lisa Yin, and Hongbo Yu. Finding Collisions in the Full SHA-1. In Shoup [42], pages 17–36.
45. Xiaoyun Wang and Hongbo Yu. How to Break MD5 and Other Hash Functions. In Cramer [9], pages 19–35.
46. Moti Yung, editor. *Advances in Cryptology - CRYPTO 2002, 22nd Annual International Cryptology Conference, Santa Barbara, California, USA, August 18-22, 2002, Proceedings*, volume 2442 of *Lecture Notes in Computer Science*. Springer, 2002.

A The amount of freedom degrees

Once a differential path settled, a point has to be clarified: the amount of freedom degrees available to the attacker. Indeed, one has to evaluate how much valid pairs can be found for the whole differential trail. We want to ensure that enough solutions for the controlled rounds exist so that we have a good probability that at least one of them will fulfill the entire differential characteristic. Moreover, when searching for semi-free-start collisions, we may even go further since we may require an important amount of valid candidates for the entire differential path.

Freedom degrees for ECHO

We use the same counting reasoning than in [15], except that we have to precisely evaluate what is the freedom degrees consumption for the various 2 AES-round differential transitions as well (in [15] it was implicitly assumed that all the BIG SubBytes transitions were $\mathtt{F} \rightarrow \mathtt{F}$, thus happening with probability very close to 1 and consuming no freedom degrees). For example, let us take the $\mathtt{D} \rightarrow \mathtt{1}$ transition through the BIG SubBytes in the forward direction: we require one AES MixColumns transition $4 \rightarrow 1$ which happens with probability 2^{-24}. Thus, if we have k valid candidates on the input, we obtain $k \times 2^{-24}$ valid candidates on the output of this layer and we consumed 2^{24} freedom degrees. The amount of freedom degrees consumed during a transition is the invert of the probability of success of this transition. Thus, with Table 2, it is very easy to compute the freedom degrees consumption for all the AES round transitions considered so far.

We illustrate the counting method by applying it to the example of the 7-round path from Figure 3. First, note that the improved Super-Sbox attack for ECHO will find **all** the possible internal states such that the controlled rounds are verified. We start from state $\mathsf{B.MC}_3^{in}$ (located between $\mathsf{B.ShR}_3$ and $\mathsf{B.MC}_3$). This state is fully filled with column differences which means that we can start with $2^{2048+32\times16} = 2^{2560}$ distinct pairs. When going forward, the $\mathsf{B.MC}_3$ transition happens with probability $2^{-24\times16} = 2^{-384}$ and the transition through $\mathsf{B.MC}_4$ happens with probability $2^{-24\times4} = 2^{-96}$. All the other layers are verified with probability one so the forward computation consumes $2^{384+96} = 2^{480}$ freedom degrees. Then, during the backward computation, the sixteen $\mathtt{C} \leftarrow \mathtt{F} \leftarrow \mathtt{D}$ transitions through $\mathsf{B.SB}_3$ happen with probability $2^{-16\times96} = 2^{-1536}$ according to Table 2 ($\mathtt{C} \leftarrow \mathtt{F}$ with probability 2^{-96} and $\mathtt{F} \leftarrow \mathtt{D}$ with probability 1). Also, the four $\mathtt{D} \leftarrow \mathtt{1} \leftarrow \mathtt{C}$ transitions through $\mathsf{B.SB}_2$ happen with probability $2^{-4\times24} = 2^{-96}$ ($\mathtt{D} \leftarrow \mathtt{1}$ with probability 1 and $\mathtt{1} \leftarrow \mathtt{C}$ with probability 2^{-24}). Then, the BIG MixColumns transitions through $\mathsf{B.MC}_2$ are verified with probability $2^{-4\times4\times24} = 2^{-384}$ and through $\mathsf{B.MC}_1$ with probability $2^{-4\times24} = 2^{-96}$. All the other layers in the backward direction are verified with probability one. Overall, the backward computation consumes $2^{1536+384+96+96} = 2^{2112}$ freedom degrees. We can finally conclude that we started with 2^{2560} pairs from which only a factor $2^{-480-2112} = 2^{-2592}$ will be valid for the whole differential path. Thus, used as is, one has to use the 128-bit salt input in order to generate 2^{96} distinct valid pairs for the 7-round path from Figure 3.

Finally, some additional freedom degrees can be obtained if one considers that the salt value can be fully controlled by the attacker. While this scenario is not very relevant in practice, it is interesting to see what the attacker is able to do in such a situation. In the case of ECHO, the salt value is 128-bit long and it then directly adds 2^{128} supplementary freedom degrees. To conclude, if he controls the salt, the attacker can generate 2^{96} distinct valid pairs for the 7-round path depicted in Figure 3. The same method is used for all the differential trails for ECHO considered in this article.

Note that the differential paths we use are just instances among a family of good differential trails. For example, in the case of the 7-round path from Figure 3, instead of placing the active word on the top left position of $\mathsf{B.MC}_0^{out}$ (between $\mathsf{B.MC}_0$ and $\mathsf{B.SB}_1$), one could place it in the 15 others locations. Those new paths present the same properties than the original one and this reasoning also applies to the active word located in $\mathsf{B.MC}_4^{out}$ (between $\mathsf{B.MC}_4$ and $\mathsf{B.SB}_5$). As a consequence, the attacker manages $16^2 = 2^8$ different core paths which provides him 2^8 additional freedom degrees.

Freedom degrees for Grøstl

The case of Grøstl is easier to analyze since we don't have to handle word-wise and byte-wise truncated differentials at the same time. Yet, the same counting technique can be applied. Interestingly, for all the paths we provided concerning Grøstl, an attacker can expect only one solution for the whole trail with good probability. This explains why one can not really hope for a semi-free-start collision attack on reduced versions of Grøstl (such as 7 or 8-round versions) with the paths given. Or, said in other words, a semi-free-start collision attack may be mounted, but will only work with a low probability.

As an example, we provide here the freedom degrees analysis for the 10-round differential path from Figure 17. By starting from the fully active internal state located at the output of MC_4, we begin with about $2^{512\times 2} = 2^{1024}$ distinct pairs of internal state values. When going forward, the first freedom degrees consuming operation is the MC_5 transition which happens with probability $2^{-7\times 56-48} = 2^{-440}$. Then, one byte is erased during AC_6 while the transition through MC_6 happens with probability 2^{-48} and in total this round consumes $2^{8+48} = 2^{56}$ freedom degrees. Finally, the last consuming operation when computing forward is AC_7 for which two bytes have to be erased (2^{16}). When computing backward, the MixColumns functions MC_3 and MC_2 requires $2^{48\times 8} = 2^{384}$ and $2^{2\times 56} = 2^{112}$ freedom degrees respectively. Then, two bytes are erased through AC_2 and all the other differential transitions consume nothing since they are deterministic. Finally, we started with 2^{1024} freedom degrees from which only a fraction $2^{-440-8-48-16-384-112-16} = 2^{-1024}$ will verify the whole differential path. Thus, since this reasoning is done on average, an attacker has a good probability to obtain one single solution for the whole differential path.

Of course, one may argue that the attacker should have one more freedom degree to perform the attack. Yet, note that until really performed, most hash function attacks only have a certain success probability to actually find a solution. For example, in the case of SHA-1, even if very low, there is a probability that the known collision attacks eventually provide no solution. Therefore, with only a single freedom degree missing, we believe that the success probability is far sufficiently high in order to consider the attack as valid. Finally, additional freedom degrees can be found by using a generalization of the internal differential attack, as explained in Section 5.5.

B Distinguishing the full internal permutation of ECHO-256

A 8-round core truncated differential path is given in Figure 12. Its usability is limited only to distinguish 8 rounds of the internal ECHO permutation (the full number of rounds for ECHO-256) and not a smaller number of rounds by cutting the beginning and/or the end of the trail. Indeed, the improved Super-Sbox attack for ECHO can not be used anymore as too many active cells are present in the middle rounds. One has to use the classical Super-Sbox method instead, which is inefficient in the case of ECHO since it requires at least 2^{512} computations and memory.

From this core trail we derive the truncated differential path from Figure 13 for which one can obtain a valid candidate with a complexity of 2^{512} computations and memory. Indeed, the uncontrolled rounds are verified with probability 2^{-480} (because of the sixteen AES MixColumns transitions $4 \rightarrow 1$ through $\mathsf{B.MC}_5$ and the four AES MixColumns transitions $4 \rightarrow 1$ through $\mathsf{B.MC}_1$), but the Super-Sbox forces a minimal cost of 2^{512}. Concerning the freedom degrees, the counting method from Appendix A shows that the attacker can generate a total of 2^{64} valid candidates for the whole differential path (and 2^{192} when the salt is controlled as well).

The solution pair has four active 128-bit words in the input and four active 128-bit words in the output (the last BIG MixColumns call is not taken in account since it is fully linear). The situation is exactly the same as for the 7-round distinguisher using path from Figure 3: by reusing the concept of *limited birthday distinguishers* [15] we deduce that for a random 2048-bit permutation, finding such a pair should require at least 2^{1024} operations.

The 8-round path from Figure 14 (also derived from the full core path from Figure 12) seems to be slightly better since the uncontrolled rounds are verified with probability $2^{-96-96} = 2^{-288}$ (because of the four D $\leftarrow$ 1 $\leftarrow$ C transitions through $\mathsf{B.SB}_5$, the four AES MixColumns transitions $4 \rightarrow 1$ through

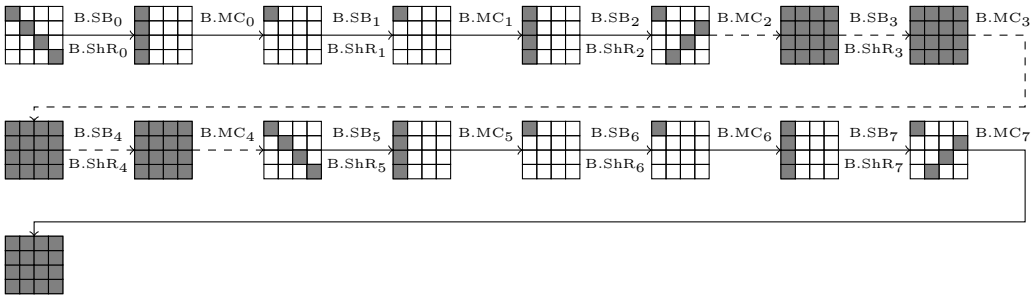

Fig. 12. Core truncated differential path for 8 rounds of the ECHO internal permutation. Each cell represents a 128-bit word and a gray cell stands for an active word. The controlled rounds are depicted with dashed lines.

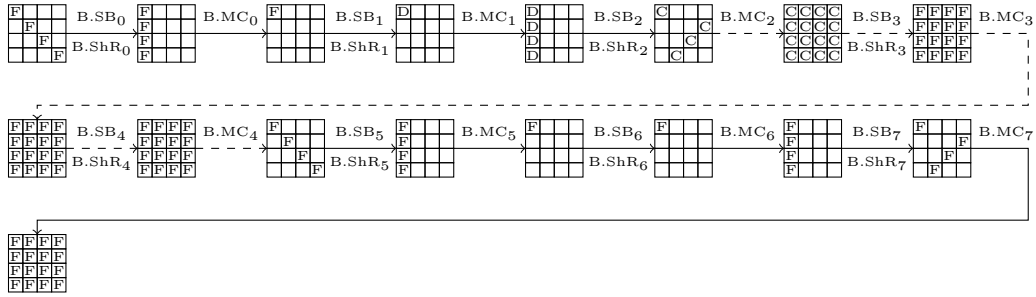

Fig. 13. 8-round differential path for the ECHO internal permutation. The controlled rounds are depicted with dashed lines.

$\mathsf{B.MC}_5$ and the four AES MixColumns transitions $4 \rightarrow 1$ through $\mathsf{B.MC}_1$). However, the amount of freedom degrees is greatly reduced as the attacker has a very small probability 2^{-128} to actually find a single valid candidate for the whole differential path. Thus, this path is acceptable only if the salt can be controlled, which would lead to a single valid pair for the whole differential trail.

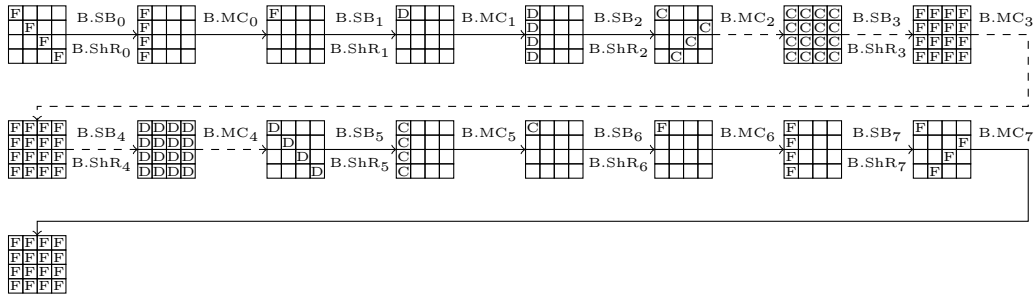

Fig. 14. 8-round differential path for the ECHO internal permutation. The controlled rounds are depicted with dashed lines.

The results concerning the internal permutation of ECHO are summarized in Table 4. Note that none of those distinguishers apply to the ECHO compression function due to the extra protection provided by the final shrinking stage of the compression function – namely its convolution effect on the output distribution of the permutation.

Table 4. Summary of results for the internal permutation of ECHO.

target	rounds	computational complexity	memory requirements	type	section
ECHO internal permutation	8	2^{768}	2^{512}	distinguisher	see [15]
	7	2^{128}	2^{32}	distinguisher	this paper
	8	2^{512}	2^{512}	distinguisher	this paper

C The ECHO-SP case

In the latest versions of the submission document [3], the authors propose a variant of ECHO, named ECHO-SP (for simple pipe). The specifications are exactly the same, but the final phase at the end of each compression function call outputs a n-bit chaining variable for a n-bit final hash value. Namely, the compression function of ECHO-SP-256 is identical to the one from ECHO-256 except that the two first words are xored with the two last words of the output column in order to obtain a 256-bit output chaining variable.

$$H' = \mathsf{comp}_{256sp}(P_E^8(H||M) \oplus H||M)$$

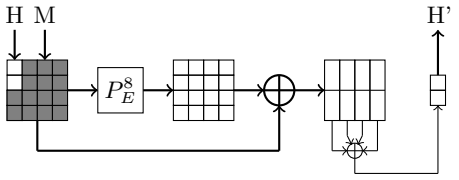

The compression function of ECHO-SP-512 is also identical to the one from ECHO-512 except that the first words column is xored with the second words column in order to obtain a 512-bit output chaining variable. Said in other words, ECHO-SP-512 and ECHO-256 compression functions are identical and the results obtained on the latter directly apply to the former.

$$H' = \mathsf{comp}_{512sp}(P_E^{10}(H||M) \oplus H||M)$$

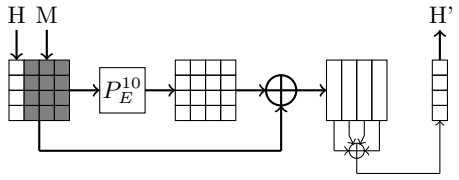

Concerning ECHO-SP-256, we use the differential path from Figure 15 which is almost identical to the one from Figure 9. The analysis is also identical and we obtain semi-free-start collisions with 2^{64} computations and 2^{32} memory. Note that one can not use the distinguishing attack from ECHO-256 anymore, because the generic complexity decreases with the output size.

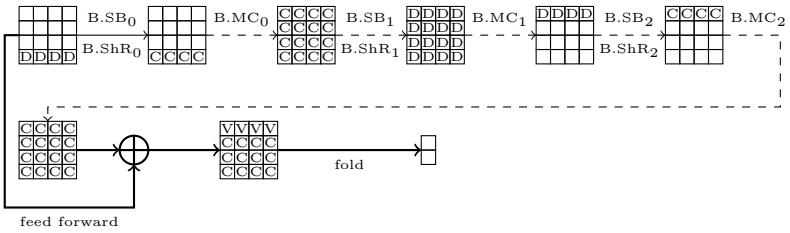

Fig. 15. 3-round differential path for the ECHO-SP-256 compression function free-start collision attack. The controlled rounds are depicted with dashed lines. We denote by V an AES word with one column and one diagonal active.

D The truncated differential paths for Grøstl

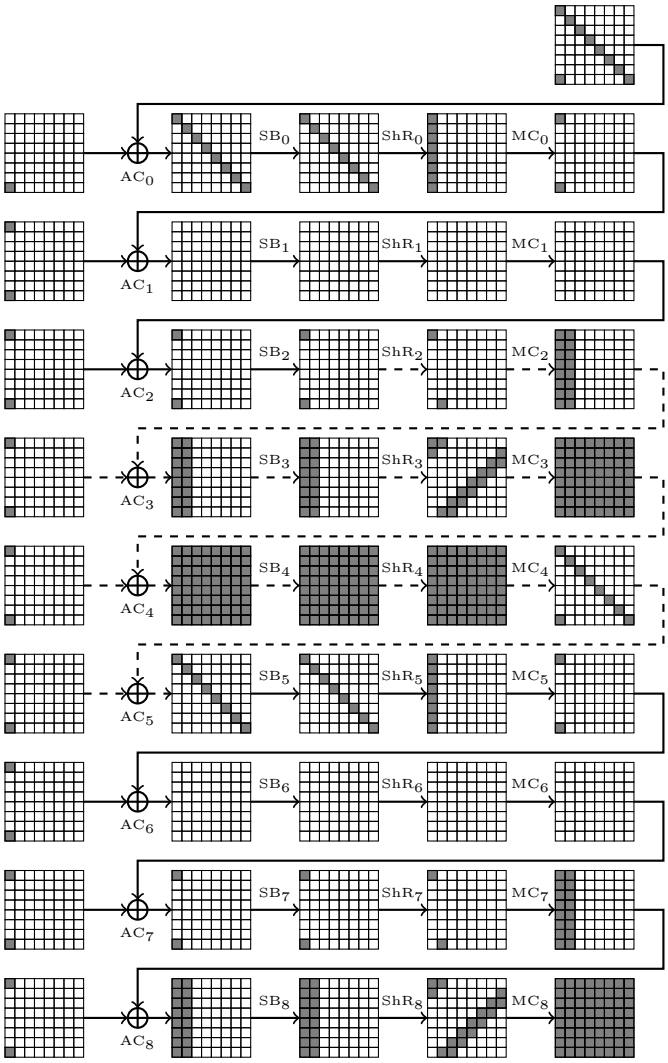

Fig. 16. 9-round differential path between P and Q for Grøstl-256. Each cell represents a byte and a gray cell stands for an active byte. The controlled rounds are depicted with dashed lines. The matrices on the left represent the differences incorporated during the AC layers.

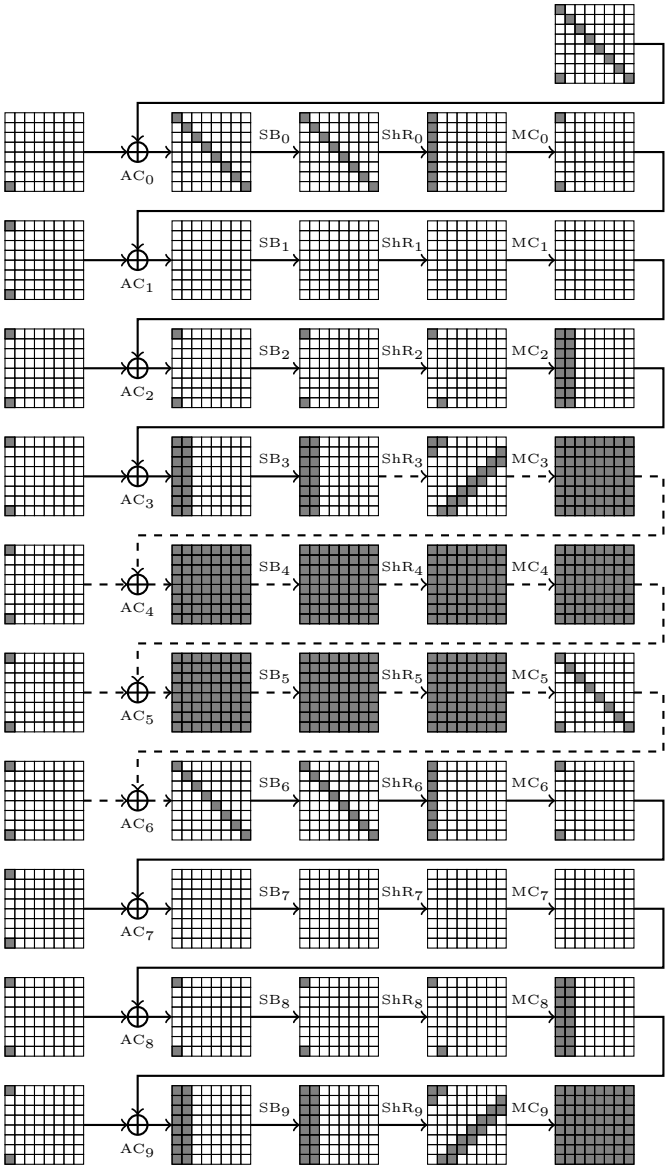

Fig. 17. 10-round differential path between P and Q for Grøstl-256. Each cell represents a byte and a gray cell stands for an active byte. The controlled rounds are depicted with dashed lines. The matrices on the left represent the differences incorporated during the AC layers.

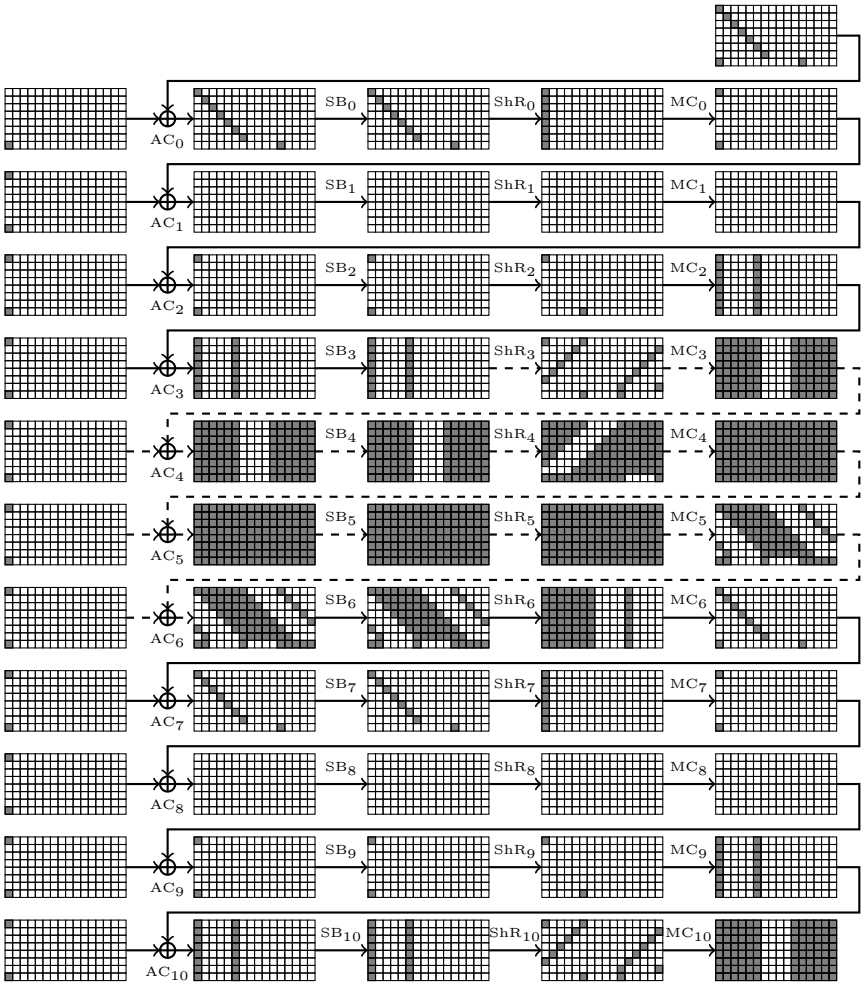

Fig. 18. 11-round differential path between P and Q for Grøstl-512. Each cell represents a byte and a gray cell stands for an active byte. The controlled rounds are depicted with dashed lines. The matrices on the left represent the differences incorporated during the AC layers.

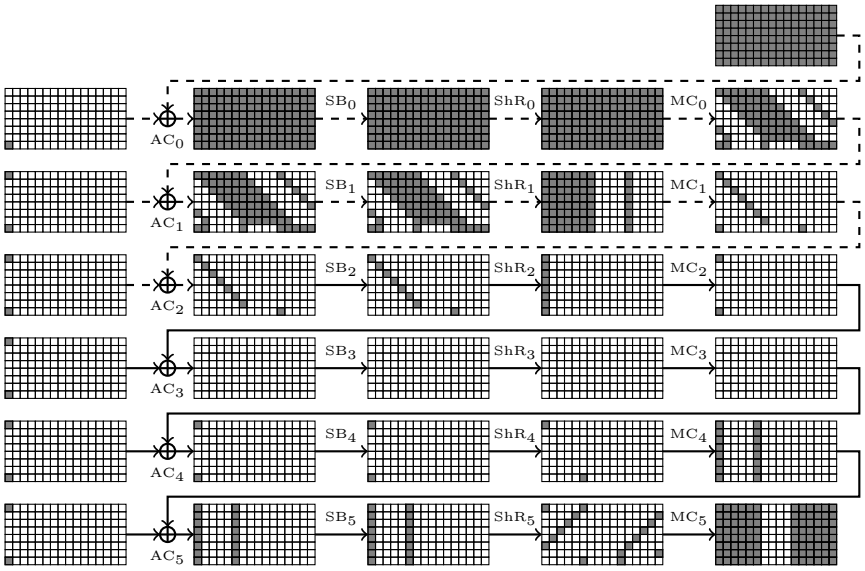

Fig. 19. 6-round differential path between P and Q for Grøstl-512. Each cell represents a byte and a gray cell stands for an active byte. The controlled rounds are depicted with dashed lines. The matrices on the left represent the differences incorporated during the AC layers.